Towards an ab-axis giant proximity effect using ionic liquid gating

Atesci, H.

Chapter 1

Introduction

Since its discovery in 1911 by Kamerlingh Onnes [1], superconductivity has been a very intriguing topic in physics. The advent of the Bardeen-Cooper-Schliefer (BCS) theory in 1957 made it possible to explain the basic mechanisms of superconductivity. The theory states that the electrons of the system undergo a bosonic transition, behaving as a single quantum mechanical wave function. The related order parameter is $\psi = \psi_0 e^{i\phi}$, where the amplitude of the wave function ψ_0 determines several key properties such as the energy gap Δ and transition temperature T_c. The highest T_c perceived to be possible ($\sim$30 K [2]) was reached with the compound Nb_3Ge in 1979 with a T_c of 23.2 K [3], which was surpassed in 1986 with the discovery of high-T_c superconductivity in the cuprate compound of $La_{2-x}Ba_xCuO_4$ with a T_c of 35 K. The subsequent discovery of many new cuprates culminated in critical temperatures as high as 150 K in $HgBa_2Ca_2Cu_3O_{8+\delta}$ only 6 years later [4]. Theoretically, it was clear that the original BCS framework was not adequate in describing this new class of compounds [2], and to this day there is no scientific consensus on the origins of some of the basic phenomenology of high-T_c superconductivity, e.g. the so-called pseudogap and the giant proximity effect. It seems that a general, BCS analog for the cuprate superconductors is even further away. Nevertheless, there is a renewed interest in the field due to improved growth techniques [5–7] and novel electrostatic charge induction mechanisms which use ionic liquids [8–11].

Among all the enigmatic issues regarding high-T_c superconductivity, this thesis aims to clarify the origins of the giant proximity effect (GPE) found in some systems where two superconductors are coupled

by a weak link, also called Josephson junctions. Hence, addressing the GPE would first involve the concept of the standard proximity effect found between a superconductor (S) and a normal metal (N). The theory concerning this issue was developed in the 1960s [12], stating that when Cooper pairs leak from S to N, the order parameter amplitude of the Cooper pairs decays exponentially away from the superconductor over a characteristic length ξ, also called the coherence length, leading to a mutual altering of the properties of both materials. For Josephson junctions, where two interfaces are present, the results are analogous to the aforementioned case of a single interface. The supercurrent between both superconducting leads with a critical temperature T_c in such SNS junctions is given by [12]

$$I_c = \frac{\pi}{2eR_n}\frac{|\Delta_0|^2}{k_B T_c}\frac{d}{\xi_n}e^{-d/\xi_n}, \tag{1.1}$$

where R_n is the normal resistance of the metal, Δ_0 is the superconducting gap in the bulk of the superconductor, d is the thickness of the normal metal, and ξ_n is the superconducting coherence length in the normal region. Here, ξ_n decreases with temperature T as $1/T$ (clean limit: $\xi_n \ll l_n$) or $1/\sqrt{T}$ (dirty limit: $\xi_n \gg l_n$), with l_n the mean free path in N.

1.1 Giant proximity effect

Not all Josephson junctions behave according to this relationship. One of the first mentions of an anomalous proximity effect in high-T_c superconductors was made in 1991 regarding co-planar junctions of the cuprates $HoBa_2Cu_3O_{7\text{-}x}/La_{1.5}Ba_{1.5}Cu_3O_{7\text{-}\delta}/HoBa_2Cu_3O_{7\text{-}\delta}$ [13]. Here, supercurrents were detected spanning over distances reaching 500 nm, two orders of magnitude larger than the theoretical value of the coherence length [14]. Other reports include co-planar Nb-BiSb-Nb junctions [15] for distances reaching 1000 nm. Others, see Ref.16, used laser light with a specific energy to photoinduce local free holes in the CuO_2 planes of $YBa_2Cu_3O_{7\text{-}\delta}$. In doing so, Josephson junctions of varying separations could be made. Long range proximity effects could be seen in junctions with separations of up to 100 nm, while the coherence length is only 15 nm. In Ref.17 oxygen ion-irradiated junctions of $YBa_2Cu_3O_{7\text{-}\delta}$ could lead to Josephson coupling over large distances (up to 880 nm) between

undamaged superconducting leads. Furthermore, in Ref.18, unconventional Josephson coupling was present in ramp-edge junctions of $Pr_{1.85}Ce_{0.15}CuO_4/Pr_{2-x}Ce_xCuO_4/Pr_{1.85}Ce_{0.15}CuO_4$, which are electron-doped cuprates. The coupling is independent of the concentration x of Ce^+ per unit cell and persists for barrier widths of up to 40 nm, approximately three times larger than the nominal coherence length. The same is not true for ramp-edge junctions of $La_{2-x}Sr_xCuO_4$ with a 50 nm thick barrier of $La_{1.95}Sr_{0.05}CuO_4$ stacked between its optimally doped electrodes [19].

The issue with the aforementioned co-planar geometric junctions is that it usually involves an ex-situ process of ion milling/damaging. This leads to a badly defined interface in terms of cation or oxygen stoichiometry, as argon ion milling tends to be a destructive process and involves oxygen vacancy production. Hence, in all of these *ab*-axis (i.e., in-plane directions, parallel to the a and b axes of the unit cell) reports, it is not clear whether the effect is intrinsic to the junction or is caused by the deficiencies in the method of preparation such as impurities by ion implantation, or interfacial effects due to improper growth techniques.

In *c*-axis geometry junctions (i.e., out-of-plane direction, parallel to the c axis of the unit cell), it is crucial that there are no superconducting shorts between the electrodes due to suboptimal growth of the barrier material. This can be caused either by superconducting shorts related to surface roughness being larger than the barrier thickness, or secondary-phase precipitates. These strict requirements were met using molecular beam epitaxy (MBE) methods. Using MBE, Bozovic *et al.* have been able to grow superlattices of $Bi_2Sr_2CuO_6/Bi_2Sr_2CaCu_2O_8$ [5] and $La_2CuO_{4+\delta}/La_{1.85}Sr_{0.15}CuO_4$ [6]. In both cases a supercurrent was found between the electrodes over distances of 10^2 times the corresponding coherence lengths along the *c*-axis in the temperature range of $T_{c'} < T < T_c$, with $T_{c'}$ and T_c being the critical temperatures of the barrier (S') and electrode (S), respectively. The observation has been coined the giant proximity effect (GPE). These reports showed that the GPE is indeed intrinsic. Similar results were found in pulsed laser deposited (PLD) $YBa_2Cu_3O_{7-\delta}/La_{2-x}Sr_xCuO_4$ superlattices [20].

Giant and anomalous proximity effects were also reported for metal superconductors [21, 22], indicating that the effect is not solely restricted to cuprate high-T_c materials, but seems to be more of a generic

Material	$\xi_{nominal}$ (nm)	L (nm)	Explanation given	Ref.
LSCO/LSCO(Sr=0.35)	$2-3$	10	Phase stiffness	[23]
LSCO(x =0.15)/LCO(4+δ)/ LSCO(x =0.15)	$0.1-0.2$	20	Resonant tunneling	[6]
LSCO(x =0.16)/LSCO(x =0.06)/ LSCO(x =0.16)	< 2.5	46	Resonant tunneling, phase pinning	[7]
YBCO/YBCO(6+δ)/YBCO	2	800	Resonant tunneling	[17]
YBCO(6+δ)/YBCO/YBCO(6+δ)	9	100	-	[16]
YBCO(6+δ)/LSCO/YBCO(6+δ)	< 1	20	Phase fluctuations	[20]
BSCO/BSCCO/BSCO	$0.1-0.3$	7.4	-	[5]
PCCO(x =0.15)/PCCO(x =0.05)/ PCCO(x =0.15)	4.5	35	-	[18]
HBCO/LBCO/HBCO	0.75	100	-	[13]
Pb+Pb/Si(111)	-	> 100	de Gennes	[21]
Nb/BiSb/Nb	-	1000	-	[15]

Table 1.1: List of long range proximity effect literature references, along with $\xi_{nominal}$, L (maximal width of the barrier that still shows a Josephson coupling) and the explanations given. Here, LSCO, YBCO, BSCO, BSCCO, PCCO, HBCO and LBCO are abbreviations for $La_{2-x}Sr_xCuO_4$, $YBa_2Cu_3O_7$, $Ba_2Sr_2CuO_6$, $Ba_2Sr_2CaCuO_8$, $P_{2-x}Ce_xCuO_4$, $HoBa_2Cu_3O_{6+\delta}$ and $La_{1.5}Ba_{1.5}Cu_3O_{6+\delta}$, respectively. If applicable, the doping levels of the respective cuprates are enclosed within parentheses.

effect of junction materials at temperatures in between both T_c's. A more comprehensive list of various literature references to the anomalous proximity effect can be seen in Table 1.1.

1.2 Schools of thought

It is important to note that until now there is no consensus on the origins of the GPE, and it is possible that different explanations apply for different systems. Some make use of conventional theoretical frameworks to explain the effect. In short, these make use of de Gennes' theory. The second type relates to the debated pseudogap physics, and several theories regarding superconducting puddles and phase pinning exist in this context. Others have come up with new mechanisms of Bose-Einstein condensation of real-space pairs [24], chiral d-density waves generated superconductivity [25], and type-II

Bose-Mott insulators.

1.2.1 Conventional de Gennes theory

Some explanations given for the GPE in the literature were given in terms of conventional de Gennes theory, as used for SN interfaces. According to Cherkez *et al.*, de Gennes already discussed the proximity effects between two superconductors with different critical temperatures and energy gaps [12], albeit qualitatively [21]. According to the authors, the local density of states of superconductors S and S' should be modified considerably in the sense that a local order is induced due to some attractive pairing interaction. The authors use the Usadel equations to quantify superconducting parameters at the interface, and find that the induced order parameter should decay exponentially as a function of the distance x from the interface, similar to de Gennes' theory:

$$\Delta \propto e^{-x/L_\Delta(T)}. \tag{1.2}$$

Here, $L_\Delta(T)$ is the temperature dependent decay length, which diverges near the $T_{c'}$ along de Gennes' theory as $L_\Delta \sim 1/\sqrt{T - T_{c'}}$. The authors of Ref.26 are of the opinion that also the results for $YBa_2Cu_3O_{7\text{-}\delta}$ can be explained with de Gennes' theory. They have put forward the idea that in most cases the $SS'S$ junctions concern one and the same material with different doping, as is the case in Ref.16. Due to this, they argue, the coupling constants of both the S and S' parts [27] of the junction are rather similar, leading to seemingly long range proximity effects. However, their suggestion does not account for the anomalous proximity effects seen in stacks of different materials, such as $YBa_2Cu_3O_{7\text{-}\delta}$ and $La_{2\text{-}x}Sr_xCuO_4$ [20].

1.2.2 Pseudogap phenomenon

When Cooper pairs are formed with a pairing energy Δ per electron, an energy gap opens in the density of states of the material, coupled to an increase of the electronic states just at the edges of the gap, which is confirmed by scanning tunneling spectroscopy [28] and other methods [29]. For high-T_c superconductors, the energy gap, however, does not disappear for temperatures higher than the critical temperature, when the material has a non-zero resistance, giving it an anomalous property, coined as the pseudogap. The exact physical origins of the

pseudogap are still unknown, but it is most apparent in underdoped cuprates (see Fig. 1.1).

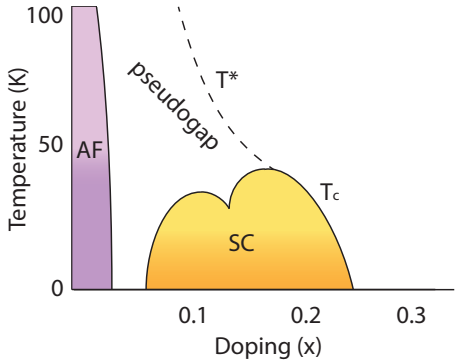

Figure 1.1: The typical phase diagram of hole-doped cuprates. Between the antiferromagnetic (AF) insulator and superconducting (SC) phases, a pseudogap is present at temperatures below T^*>T_c, primarily in the underdoped regime.

According to some, the pseudogap represents a mixture of phases combined with the superconducting phase [30]. Others view the pseudogap as signifying preformed pairs as a precursor to superconductivity, which acquires global phase coherence only below T_c [31].

The latter is derived from the idea that amplitude and phase are the main parameters that describe the order parameter. The formation of Cooper pairs is not sufficient to induce superconductivity, as the pairs need to condense into a phase coherent quantum mechanical state [32]. Hence, this picture makes use of the competition between amplitude (i.e. pairing) and phase to account for the large pseudogap in underdoped cuprates. According to this view [32], pairing may dominate at low doping levels where the system is homogeneous. The large energy scale of pairing in the underdoped cuprates leads to a high pairing temperature T_p (see Fig. 1.2), which gets reflected in the pseudogap. Electronically, the material is spatially inhomogeneous and this inhomogeneity is followed by the order parameter, leading to a non-zero resistance. In particular, the phase stiffness of the order parameter is weakened and becomes susceptible to fluctuations. The phase fluctuations tend to decrease the phase ordering temperature T_θ [33], while the system transforms to a phase ordering regime when

increasing the inhomogeneity through doping, leading to an increase (decrease) in T_θ (T_p). Hence, optimal T_c is found at intermediate doping levels.

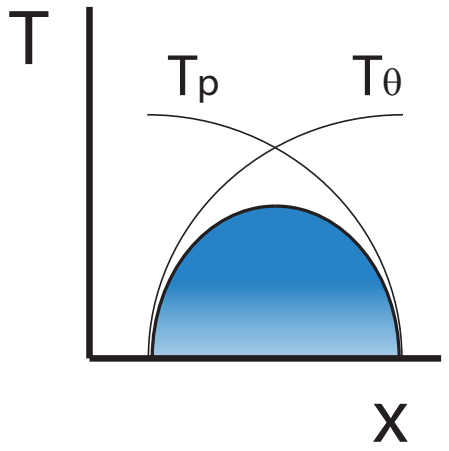

Figure 1.2: Phase diagram belonging to the physics of preformed pairs. The interplay between the pairing (T_p) and phase ordering (T_θ) temperatures as a function of doping x leads to an optimal critical temperature T_c at intermediate doping levels [32].

With this picture in mind, introducing phase stiffness in an underdoped cuprate provides the necessary ingredient to optimization of T_c. The necessary phase coherence can be provided by superconducting metals [34], or cuprates with large phase stiffness, present in either the superconducting regime [7] or the overdoped regime [23]. Consequently, Yuli *et al.* [23] reported substantial increases in T_c for underdoped $La_{2-x}Sr_xCuO_4$ films in the range of $x = 0.05-0.125$ when an overdoped layer of $La_{1.65}Sr_{0.35}CuO_4$ is grown as a capping layer. The authors mention that the effect is not attributable to strain effects or intermixing of Sr cations or oxygen within the layers. Rather, they suggest that the overdoped $La_{2-x}Sr_xCuO_4$ quenches the phase fluctuations present in the underdoped material, leading to larger phase stiffness and hence an enhancement of T_c in overdoped-underdoped multilayers. This approach is capable of explaining phase coherence effects in more generic systems which include non-cuprate superconductors as well, such as granular Pb films covered by a layer of Ag

[22].

The same argument can be used to explain the giant proximity effect in $SS'S$ junctions [35]. The critical current dependence on the temperature and barrier width is found to be qualitatively different than in the standard SNS case. More specifically, the effective T_c of the junction is predicted to behave as

$$T^{eff} \cong T_c \left[1 - \left(1 - \frac{T_{c'}}{T_c}\right) \frac{ln(d/\xi)}{ln(L/\xi)}\right]. \tag{1.3}$$

Here, d, ξ and L stand for the barrier width, the coherence length and length of the superconducting leads, respectively. T_c and $T_{c'}$ represent the critical temperature of the S and S' layers, respectively. These are proportional to their nominal critical temperatures. According to Ref.35, the giant proximity effect is visible for length scales smaller than the magnetic penetration depth λ. In light of the theory proposed, this should coincide with a ratio of $\ln(d/\xi)/\ln(\kappa)$ that is sufficiently small, preferably below unity. Here, $\kappa = \lambda/\xi$, which for cuprates in the order of 10^2 - 10^4.

1.2.3 Superconducting puddles

Some theoretical works have made attempts to explain the giant proximity effect in light of inhomogeneous barriers [36, 37], in which the barrier material is considered to contain pockets of superconductivity. This concept is rooted in the preformed pairs picture of the pseudogap phase. Covaci *et al.* proposed that this is due to interstitial oxygen dopants, which enhance the pairing interaction locally [38]. Hence, these superconducting clusters will be linked through the proximity effect, leading to a current through the percolative paths, coupling the superconducting electrodes [39]. This is comparable to statements in Ref.36, in which a theoretical framework of the giant proximity effect was made by assuming an inhomogeneous nature of the barrier material. Here, superconducting islands are imbedded in a metallic matrix. This allows Cooper pairs to tunnel resonantly through a series of superconducting islands, comparable to what is stated in the works of Bozovic *et al.* [6]. The percolation-like interpretation should lead to the typical critical order parameter seen in percolation-driven conduction. Hence, the critical current I_c measured between the superconducting leads, is predicted to behave accordingly as [36]

$$I_c \propto (T/T_c - 1)^{\nu}, \tag{1.4}$$

where ν is the well-known critical index value of 4/3 in percolation theory.

1.3 Novel theoretical explanations

1.3.1 Mott insulators

The concept of Mott insulators was introduced in 1949 [40], which stated that some materials that should be metallic according to standard band theory are insulating due to strong Coulombic electron-electron repulsive interactions. These effects are reported to become prominent in systems where the dimensionality of the system is reduced, such as one-dimensional GaAs wires, or undoped two-dimensional high-T_c superconductors [41]. The basic electronic characteristics of the cuprates is described using the archetypical cuprate $La_{2-x}Sr_xCuO_4$, the crystal structure of which is seen in Fig. 1.3a. Here, the CuO_2 planes are separated by charged reservoir layers. The insertion of Sr into the charged reservoir layers changes the charge carrier density of the planes. The Cu $3d$ or O $2p$ bands of the CuO_2 planes are the lowest in energy, hence responsible for the macroscopic electronic properties such as high-T_c superconductivity.

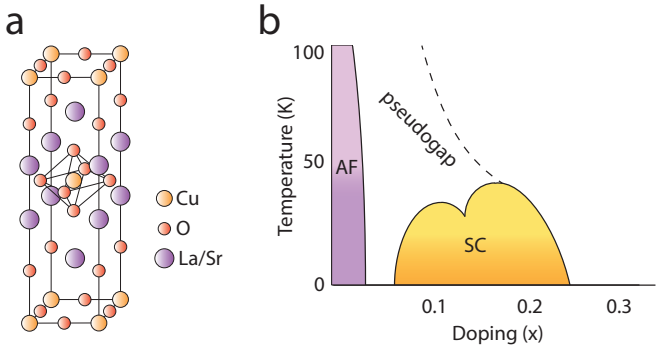

Figure 1.3: **(a)** The body-centered tetragonal structure of $La_{2-x}Sr_xCuO_4$ and **(b)** its phsase diagram. Different phases (antiferromagnetic (AF), superconducting (SC) and pseudogap) are present, depending on the temperature and doping.

The undoped compound La_2CuO_4 has an odd number number of electrons per unit cell, which under band theory conditions would

be metallic. This is clearly not the case, as the compound is an antiferromagnetic (AF) insulator. This is due to the on-site electron repulsion U dominating over the hopping energy t, leading to a split in the conduction band. This scenario applicable is for $x = 0$ in the phase diagram of Fig. 1.3b. Introducing a certain concentration x of Sr^{2+} per unit cell as substitute for La^{3+} in the charge reservoir layers leads to holes in the CuO_2 planes of the material. This destroys the AF phase of the material until the pseudogap state is reached at high enough x. Increasing x further leads to superconductivity and eventually to a Fermi liquid-like phase.

1.3.2 Type-II Bose-Mott insulators

The phase of interest in this case is the superconducting one. Its main signatures are zero resistivity and the so-called Meissner state. In the latter state, the external magnetic field is expelled from the material completely. However, this is only valid for superconductors of type I, conventional superconductors such as Al, Hg and Pb. Type II superconductivity includes nearly all compound superconductors and behaves similarly to its type I counterpart only up to a critical magnetic field H_{c1}, after which the magnetic field penetrates the material, albeit in the form of magnetic flux quanta of $\Phi_0 = 2.07 \times 10^{-15}$ Tm^2 ordered in a vortex lattice. Only above a critical field $H_{c2} > H_{c1}$ does the superconductivity disappear (see Fig. 1.4a).

Making use of the concept of duality, Beekman and co-workers developed a stand-alone theory for the investigation of Bose-Mott insulators. Surprisingly, the theory offered new opportunities for interpreting the GPE [42]. Simply put, superconductors expel the external magnetic field, while insulators expel electrical currents. Superconductors of type II above a certain critical magnetic field H_{c1} allow for the penetration of the magnetic field in magnetic flux quanta Φ_0, leading to Abrokosov vortices. On grounds of duality, something similar should happen in its type II insulating analog, but now for the electrical current. Above a critical current, the insulator should allow for the penetration of this current, in the form of quantized supercurrent filaments (see Fig. 1.4b).

According to this theory, the main parameter which determines the phase transitions is the quantum disorder, expressed as U/J with $J = 4t^2/U$, the hopping parameter in the Bose-Hubbard Hamiltonian. At one end of the U/J spectrum, i.e. $U/J \to \infty$ the on-site repulsion

dominates and the insulating phase shows up (see Fig. 1.4c), albeit of Type I. Lowering U/J to intermediate values induces a change to a Type-II Bose-Mott insulator. A further decrease leads to crossing over the quantum critical (QC) point and eventually to the familiar superconducting regimes.

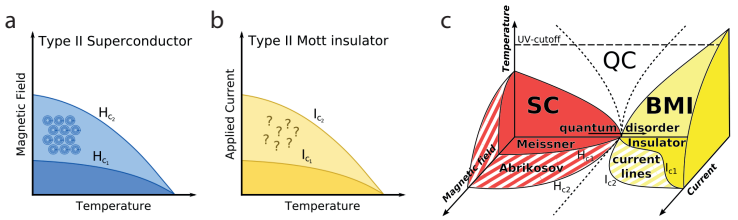

Figure 1.4: **(a)** Phase diagram of a typical type-II superconductor. For $H < H_{c1}$ the Meissner effect is present, while for $H_{c1} < H < H_{c2}$ the external magnetic field penetrates the material in magnetic flux quanta, leading to vortices. The superconducting state is cancelled for $H > H_{c2}$. The insulating analog of the type-II superconductor is the type-II Bose-Mott insulator, the phase diagram of which is shown in **(b)**. For $I < I_{c1}$ no external current is present in the material, which is not the case for $I_{c1} < I < I_{c2}$, where the current penetrates in quanta. **(c)** Phase diagram of the proposed type-II Bose-Mott insulator as a function of temperature, quantum disorder U/J and applied field and current. Adapted from [42].

The charge carriers in the material described by Beekman and Zaanen are bosons, similar to the Cooper pairs in superconductors, except that these experience a large amount of on-site, Mott-like repulsion. Hence, these materials are called type-II Bose-Mott insulators at intermediate U/J levels, or as U/J is controlled by doping, at intermediate doping levels as well. This suggests that the type-II Bose-Mott insulator could be found in the pseudogap phase where both the bosonic attraction and the electrostatic repulsion of electrons play a role, which can be found at approximately $x = 0.05$ for $La_{2\text{-}x}Sr_xCuO_4$.

Some crude estimates can be made regarding the quantum of current. It should be noted that while Φ_0 is a universal constant, the same cannot be said about the current quantum I_0. It is dependent on material properties such as phase velocity c_{ph} and the lattice parameter a. Its precise formulation is given by

$$I_0 = \frac{4\pi e c_{ph}}{a}. \tag{1.5}$$

Here, e is the electron charge. Approximating c_{ph} by the Fermi velocity (equal to 2.7×10^5 m/s) and using $a = 3.9$ Å results in $I_0 = 1.4\times10^{-3}$ A. These current quanta of I_0 are carried in filamentary structures and have a width given by the so-called Mott proximity depth,

$$\lambda_M = \lambda_L \left(\frac{c_{ph}\mu_0 e^2}{\hbar \Phi_\infty^2} \right)^{1/2}, \tag{1.6}$$

where λ_L is the London penetration depth. μ_0 is the magnetic permeability of free space and Φ_∞ is a dimensionless constant in the order of unity. Estimations have shown that this is up to two orders of magnitude smaller than λ_L [19].

If we take the aforementioned current quantum along with a typical critical current density of $1\times10^9 \mathrm{A/m^2}$ in $La_{2-x}Sr_xCuO_4$, the width of the filament would have to be at least $\sim$1 μm wide, which requires λ_L to be very large. This would only be possible when this parameter starts to diverge near the superconducting phase transition.

The energy cost of the formation of a supercurrent filament would be linear in length. Therefore, the authors argue, the current can be carried across a significant length scale, and may offer an alternative explanation for the giant proximity effect.

1.4 Outline of the thesis

The theory developed by Beekman and Zaanen offers the possibility of an interesting new phase of matter that has not yet been discovered. A first possible area to search for such a new phase is in the pseudogap region of doping of high-T_c superconductors, which formed the initial starting point of the research project of this thesis.

The present theoretical framework offered by the authors provides a partial guide since it has a number of crucial unknowns, prime examples of which include the effects of finite temperatures on the current filaments. Furthermore, the theory assumes that the current quantum filaments enter into the type-II Bose-Mott insulator isotropically, while the distribution of charge carrier density in cuprates such as $La_{2-x}Sr_xCuO_4$ is concentrated at the copper-oxide layers and is hence very much two-dimensional. In addition, the finite thickness of the films might lead to difficulties in the hypothetical formation of the filaments in the ab-axis, as λ_M is in the order of 10 nm. Therefore we

took the pseudogap phase as our starting point and focused on the interpretation of the mechanism for giant proximity effect.

Material-wise, a material is needed with an accessible phase diagram. For this requirement the cuprate $La_{2-x}Sr_xCuO_4$ is preferred. This has to do with the uniqueness of the $La_{2-x}Sr_xCuO_4$ system in that by simply changing the Sr concentration (albeit with some small oxygen non-stoichiometric possibilities), the whole of the phase diagram can be traversed. Furthermore, its crystal structure is the simplest among its cuprate counterparts with single CuO_2 layers [43]. In view of the sensitivity of the giant proximity effect to various growth inhomogeneities and imperfections, the material should be grown homogeneously and single-crystalline. Again, $La_{2-x}Sr_xCuO_4$ fits perfectly in this picture, as this has already been demonstrated by Bozovic and co-workers [6].

Based on the enhancement in the order of 10^2 of the distance over which Josephson coupling can be obtained in the *c*-axis in the experiments of Bozovic, the proximized effects should be observable for distances up to 400 nm in the *ab*-axis, as the coherence length is 3.2 nm.

In order to clarify the nature of the giant proximity effect, a number of experiments can be set up to differentiate between the applicability of the theories. This would mean that the behavior of three main junction parameters $T_{c'}$, I_c and ξ would have to be investigated qualitatively, and if possible, quantitatively as a function of barrier properties such as length L and temperature T.

Hence, in order to investigate the giant proximity effect in the *ab*-axis, a junction area has to be in its pseudogap phase, connected to superconducting leads. To pursue this, a number of methods are proposed and applied. The first proposal, as is described Chapter 8, makes use of ionic liquid gating on an initially superconducting film with a low T_c, indicated as S in (Fig. 1.5a). With this method, the gating is not applied everywhere on the film as an artificial junction area is made as the gating effect on top of this area is blocked by means of a barrier. The increased carrier density on the gated areas leads to a higher T_c, indicated as S'. Hence, the junction area at some point in temperature is in its pseudogap phase while the leads are still superconductors. The great advantage of this approach is that it allows creating a junction in a film that is structurally homogeneous. As this is a rather novel technique, the fundamentals of

ionic liquid gating based on a thorough literature study is discussed in Chapter. 2. On the experimental side, the goal of mastering the ionic liquid gating technique lead us to perform experiments on various oxide materials such as $SrTiO_3$ (Chapter 4), $Nd_{2-x}Ce_xCuO_4$ (Chapter 5) and $La_{2-x}Sr_xCuO_4$ (Chapter 6).

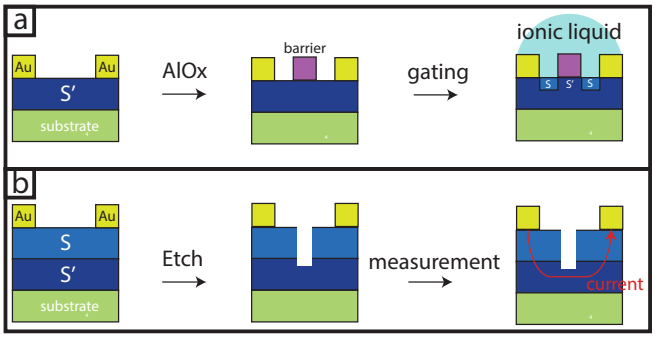

Figure 1.5: A schematic of two used methods of obtaining an *ab*-axis Josephson junction. **(a)** Ionic liquid gating-based Josephson junction. Here, the gating elevates the initial T_c. The barrier blocks the gating in the junction area. **(b)** The etched bilayer-based Josephson junction. The etched bilayer ensures that the flow of electrons between both S leads goes through the S' layer.

The second method makes use of etched bilayers, and is described in detail in Chapter 7. In short, this method involves the deposition of a film of low $T_{c'}$ (denoted as S'), followed by one of high T_c (denoted as S), see Fig. 1.5b. Etching away the top layer ensures that the flow of electrons between both S is through the S' area. The main advantage of this method is that the Δ T_c can be much higher than in the former method, as the top layer can be freely chosen. Furthermore, any electrochemical effect induced by the ionic liquid gating in the first method is circumvented in the etched bilayers. A disadvantage, however, is that the etched depth is not constant, as the top layer and interfacial layer between the top and bottom layers have some roughness. Hence, the etched depth needs to be increased to ensure that the top layer is completely etched away over the entire width of the junction area. Furthermore, the etching process leaves some disorder in the etched layer. For most hole-doped cuprates, this leads to a non-superconducting layer, the thickness of which is typically in

the order of a few nm. A more important note is that the coherence length in cuprates is anisotropic, with the *c*-axis component usually smaller by an order of magnitude or more. Hence, if the etching depth is too much, this can annul any potential proximity effect between the superconducting leads.

The thesis is finalized with an outlook on the origins of the GPE based on key measurements made with both methods in Chapter 9.